European Review for Medical and Pharmacological Sciences 2017; 21: 560-568

The expression and significance of IL-6, IFN-γ, SM22α, and MMP-2 in rat model of aortic dissection

Y.-L. CAI, Z.-W. WANG

Department of Cardiovascular Surgery, Renmin Hospital of Wuhan University, Wuhan, Hubei Province, P.R. China

Abstract. – OBJECTIVE: To examine the expression of interleukin-6 (IL-6), interferon-γ (IFN-γ), smooth muscle 22α (SM22α), and matrix metalloproteinase-2 (MMP-2) and their possible roles in aortic dissections (AD).

MATERIALS AND METHODS: Male SD rats (3 weeks) were induced for AD using 0.25% β-aminopropionitrile (BAPN) treatment for 6 weeks and were subsequently divided into the model I (with AD) and model II (no AD). Aorta was separated and observed, while TUNEL staining observed apoptosis of aortic vascular smooth muscle cells. Immunohistochemistry (IHC) staining measured the positive expression of IL-6, IFN-γ and MMP-2 in aorta tissues, followed by Western blotting for protein expressions of IL-6, IFN-γ, SM22α, MMP-2, and signal transduction factors phosphorylated c-Jun N-terminal kinase (*p*-JNK) and p-c-Jun.

RESULTS: Under an 80% rate of AD formation in model rats, those with AD had significantly higher aorta diameter and apoptosis of aortic vascular smooth muscle cells compared to those without AD or control rats ($p<0.05$). Elastic fiber gap of model I group was increased, accompanied with elastin fiber breakage and disarrangement. Model rats had significantly higher IL-6, IFN-γ, MMP-2, p-JNK, and p-c-Jun expression than control ones, and lower SM22α expression. No significant difference has been found for these parameters between model I and model II subgroups ($p>0.05$). There were significantly positive correlations between IL-6 versus MMP-2, IL-6 versus p-JNK, IFN-γ versus MMP-2, IFN-γ versus p-c-Jun in the model I group ($p<0.05$).

CONCLUSIONS: IL-6, IFN-γ, and MMP-2 expressed highly in AD. During AD formation, IL-6 and IFN-γ may enhance MMP-2 expression and increase extracellular matrix degradation of aorta vascular wall via JNK signal pathway. The apoptosis and phenotype transformation of vascular smooth muscle cells is likewise correlated with AD formation.

Key Words:
Aortic dissection, Matrix metalloproteinase-2, Interleukin-6, Interferon-γ, SM22α.

Introduction

An aorta aneurysm is one severe vascular disease and is featured with apoptosis of vascular smooth muscle cells in the aortic media, endothelial cell injury, degradation and pathological remodeling of the extracellular matrix. Currently, the etiology or pathogenesis of an aorta aneurysm has not been fully illustrated[1,2]. Some studies showed the important role of proliferation, differentiation, and apoptosis of vascular smooth muscle cells and inflammatory cells in the pathogenesis and progression of the aorta aneurysm[3,4]. The infiltration of inflammatory cells in human aneurysm tissues is positively correlated with an injury of the abdominal aorta matrix. Inflammatory cell infiltration exists since the early phase of aneurysm formation. Species and activity of matrix metalloproteinases (MMPs) and the injury conditions of collagen and elastin are elevated with severer infiltration of inflammatory cells, indicating the important role of MMPs secreted by inflammatory cells in the occurrence and progression of the abdominal aorta aneurysm[5,6]. Under focal inflammatory stimuli, inflammatory cells have elevated expression, plus enhanced MMPs secretion by vascular smooth muscle cells to damage elastin, collagen, extracellular matrix, and to induce atherosclerosis or vascular injury. During these pathological processes, the phenotype of vascular smooth muscle cells may change as smooth muscle 22α (SM22α); and SMα-myosin genes were suppressed in atherosclerosis patients, accompanied with elevated MMPs expression[7,8]. Thoracic aorta aneurysm (TAA) and thoracic aorta dissection (TAD) are major lethal diseases in vascular surgery. Their major pathological features are tumor-like dilation of the thoracic aorta, and important etiology factors include weakness of aorta walls and abnormal hemodynamics. A

Corresponding Author: Zhiwei Wang, MD; e-mail: zhiweiwangzxc@sina.com

similar pathological mechanism exists among TAA, TAD, and abdominal aorta aneurysm. Some studies showed the close correlation between inflammatory response and abdominal aorta aneurysm, as it involves the formation of TAA and TAD. This can be corroborated by elevated expression of interleukin-1β (IL-1β) and IFN-γ[9,10]. Due to double the number of elastic lamina in the thoracic aorta compared to the abdominal aorta in normal humans, inflammation with a similar condition may have differential effects on the pathology of the abdominal and thoracic aorta. Owing to the similarity between TAA and TAD, this study established a rat AD model, on which expression levels of IL-6, IFN-γ, SM22α, and MMP-2, p-JNK, and p-c-Jun were measured to investigate AD-related pathogenesis.

Materials and Methods

Animals

A total of 30 male SD rats (3 weeks old, body weight 49-51 g) were provided by the Laboratory Animal Center, Wuhan University (Certificate No. SYXK-2013-0025). Rats were singly housed in a SPF grade facility with food and water ad libitum. Animals were randomly divided into control (N=10) and model group (N=20). Rats were used for all experiments, and all procedures were approved by the Animal Ethics Committee of Renmin Hospital of Wuhan University.

Test Drugs and Reagents

β-aminopropionitrile (BAPN) was purchased from Sigma-Aldrich (St. Louis, MO, USA). Chloral hydrate and paraformaldehyde were purchased from Kemiou Chem (Tianjin, China). Rabbit anti-mouse IL-6, IFN-γ, SM22α, MMP-2, p-JNK, and p-c-Jun antibodies were purchased from Boster (Wuhan, China). Horseradish peroxidase (HRP) labeled goat anti-rabbit secondary antibody was supplied by CST (Boston, MA, USA). Electrophoresis and transfer apparatus was supplied by Bio-Rad (Hercules, CA, USA).

Animal Model

After 3 days acclimation, animals were randomly assigned into groups. Control rats received normal food and water, while the model group received 0.25% BAPN in a normal diet with water ad libitum for 6 consecutive weeks as previously reported[10]. Animal weight was monitored each week. Died animals were immediately dissected, and those survived were sacrificed after 6 weeks. Full-length aorta (from the root to the abdominal aorta-iliac artery branch site) was extracted. Those rats complicated with AD were assigned into the model I group, while those without AD were assigned to model II group. After removing loosening connective tissues, abdominal and thoracic aorta was separated.

Measurement of Aorta Diameter and Aortic Media Thickness

Aorta tissues were firstly rinsed in Green Lotion, dried and were weighted. Diameter and length of AD were measured, along with formation rate of AD, and range of dissection rupture. The thickness of the aortic media was measured in an inverted phase contrast microscope. An average value was calculated based on eight different orientations.

Morphology Alternation

AD tissue samples from AD model rats were immersed in paraformaldehyde, embedded into paraffin sections (5 μm thickness), and were stained by HE method. Under light field microscope, AD formation was confirmed. For those samples without AD formation, observation was initiated from the descending branch of the aorta. The formation of AD was determined by the same strategy on the abdominal aorta.

IHC Staining for Positive Expression of IL-6, IFN-γ, and MMP-2

Tissue samples were prepared for paraffin sections (8 μm thickness). After dewaxed, tissue sections were rinsed in phosphate buffered saline (PBS, PH 7.4) for three times (3 min each), followed by antigen retrieval. One drop of 3% H_2O_2 was added for 10 min incubation at room temperature to block endogenous peroxidase activity. A primary antibody against IL-6, IFN-γ or MMP-2 (1:100 dilution) was added for 2 hours room temperature incubation. Polymer enhancer was added and incubated for 20 min at room temperature, with the addition of enzyme labeled anti-mouse/rabbit polymer. After 30 min room temperature incubation, freshly prepared DAB buffer was added for 5 min development under the microscope, followed by hematoxylin counter staining, 0.1% HCL differentiation, tap water rinsing and drying in gradient ethanol. Tissue sections were immersed in xylene and were mounted with neutral buffered resin. Expression level was observed and analyzed in Image-pro plus system.

Western Blotting for Measuring Aorta Expression Levels of IL-6, IFN-γ, SM22α, MMP-2, p-JNK, and p-c-Jun

Rat aorta tissues were firstly lysed in the lysis buffer. The lysate was collected by centrifugation and was quantified using the BCA kit. Protein samples were separated using 10% sodium dodecyl sulphate-polyacrylamide gel electrophoresis (SDS-PAGE) gel and were transferred to polyvinylidene fluoride (PVDF) membrane. Non-specific background was removed for 1 hour, followed by the addition of anti-IL-6 (1:200 dilution), anti-IFN-γ (1:200), anti-SM22α (1:400), anti-MMP-2 (1:200), anti-p-JNK (1:200), anti-p-c-Jun (1:200) or anti-β-actin (1:1000) antibody in 4°C overnight incubation. The next day, the membrane was rinsed in PBST for three times and incubated with secondary antibody (1:1000) for 1-hour incubation. After PBST rinsing, ECL reagent was used to develop the membrane, followed by exposure under X-ray. Quantity One software (Bio-Rad, Hercules, CA, USA) was used to scan band density. Relative expression level was shown as the ratio of targeted protein bands against internal reference protein.

TUNEL Assay Apoptosis of Aorta Vascular Wall Smooth Muscle Cells

Tissue sections were de-waxed, dehydrated, and digested in Proteinase K at room temperature. The section was blocked in methanol-H_2O_2 solution, followed by PBS washing twice. The section was incubated in balanced buffer for 1 hour under room temperature, followed by the addition of TDT enzyme for 1-hour incubation at 37°C. The reaction was halted by quenching buffer for 10 min at room temperature, followed by PBS rinsing twice. Peroxidase was added for 30 min room temperature incubation, followed by DAB development. Methyl green was used in counter staining, followed by tissue dehydration and mounting. A light field microscope was used to observe tissues, followed by Image-pro plus analysis. 10 randomly selected fields (200× magnification) were used for calculating the apoptotic index (AI) or proliferation index (PI), which was calculated as the average optical density times percentage of positive cells.

Statistical Analysis

SPSS20.0 software (SPSS Inc., Chicago, IL, USA) was used for analyzing data, of which measurement data were firstly tested for normality. Those fitted normal distributions were presented as mean ± standard deviation (SD). Analysis of variance (ANOVA) was used to compare means among multiple groups, followed by LSD test in groups. Analysis of covariance (ANOVA) was used to evaluate the correlation between IL-6, IFN-γ and MMP-2, p-JNK, and p-c-Jun in the model I group. Statistical significance was defined when $p<0.05$.

Results

General Condition and Aorta Diameter of Model Rats

A total of 16 rats had AD (80% formation rates). Control rats had normal feeding and drinking behavior during the experiment, plus normal general conditions. Their body weight gradually

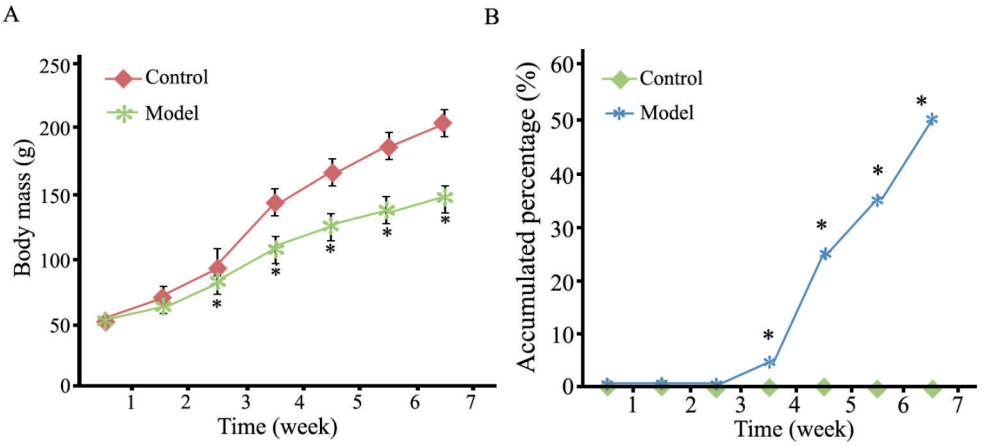

Figure 1. Body mass ***(A)*** and accumulated death rate ***(B)*** of AD model and control rats. *, $p<0.05$ compared to control group.

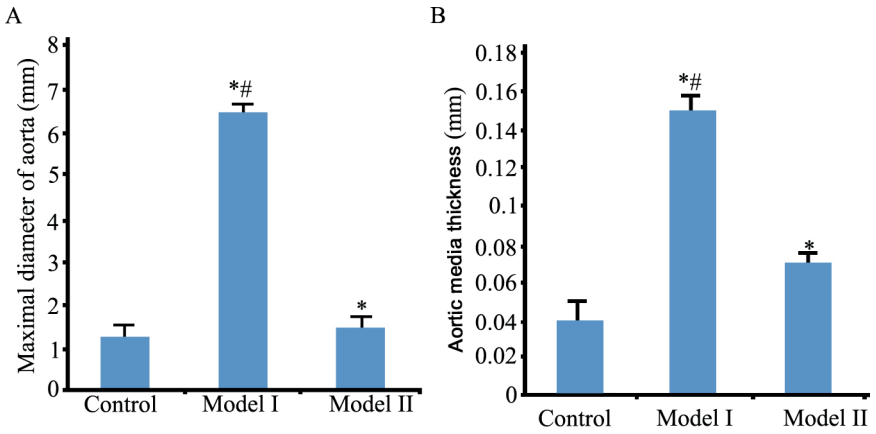

Figure 2. Aorta diameter ***(A)*** and aortic media thickness ***(B)*** of rats. Model I, rats with AD; Model II, rats without AD. *, $p<0.05$ compared to control group; #, $p<0.05$ compared to model II group.

increased with time elapsed, without AD formation. Model rats had a lower amplitude of the body weight increase compared to control group. A total of 10 rats died due to AD during experiment, with average dead time 30 ± 6 days after BAPN treatment. Dissection of dead mice showed blood clots in the chest cavity, with AD formation in the thoracic aorta (3 cases in aorta arch, 2 cases in ascending aorta, 3 cases in the proximal descending aorta, and 2 cases in ascending aorta to middle descending aorta). No abdominal AD was formed in either control or model rats. The model I group had significantly larger aorta diameter and aortic media thickness compared to model II or control group ($p<0.05$). No statistical significance existed between model rats without AD or control rats (Figures 1, 2 and 3).

Pathology and Morphology of Aorta Tissues

HE staining showed dilated aorta cavity in model rats, with aneurysm-like morphology. Victoria blue staining showed regular arrangement of elastic fibers in rat aorta tissues without rupture. After AD formation in model rats, disorganization or discontinuous segments of elastic fibers were visible, and elastic fiber gap was increased, which contains abundant erythrocytes to form a pseud-cavity, indicating blood inside AD cavity (Figures 4 and 5).

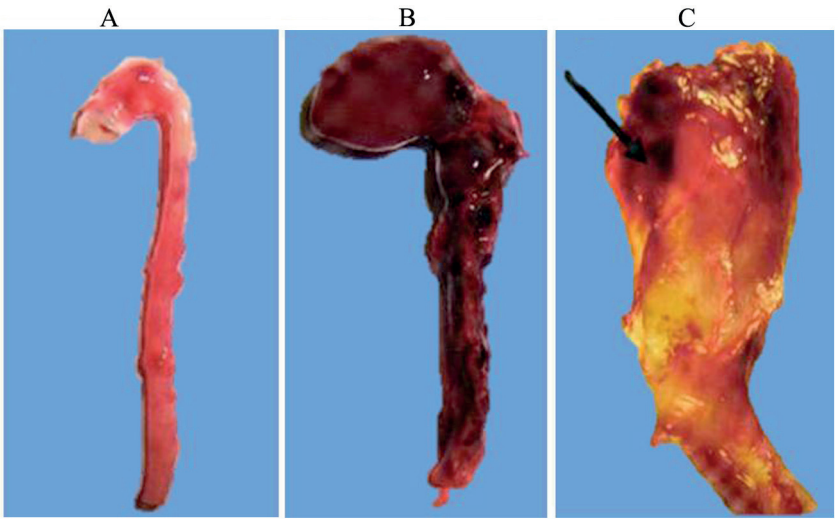

Figure 3. General observation of rat AD. ***A,*** Control group, no AD formation. ***B,*** Model I rats with AD. ***C,*** Model II rats with pseud-AD cavity.

Figure 4. H&E staining of rat aorta (×4). ***A,*** Control group, no AD formation. ***B,*** Model I rats with AD. ***C,*** Model II rats with pseud-AD cavity.

IHC Staining for IL-6, IFN-γ, and MMP-2 Expression

Elastin was presented as light blue, and nucleus was stained with dark blue. Cellular expression of IL-6, IFN-γ, and MMP-2 were shown as yellow-brown. IHC staining results showed elevated positive expression of IL-6, IFN-γ and MMP-2 than the control group (Figure 6).

Western blotting for IL-6, IFN-γ, SM22α, MMP-2, p-JNK, and p-c-Jun expression

Aorta expressions of IL-6, IFN-γ, MMP-2, p-JNK, and p-c-Jun were significantly elevated in AD model rats compared to control group, while SM22α expression was significantly depressed ($p<0.05$). No significant difference of IL-6, IFN-γ, SM22α, MMP-2, p-JNK and p-c-Jun expression level existed between model rats with and without AD formation ($p>0.05$, Figures 7 and 8). In model rats with AD, it was evident that the expression levels of IL-6 versus MMP-2, IL-6 versus p-JNK, IFN-γ versus MMP-2, IFN-γ versus p-c-Jun were significantly positively correlated ($p<0.05$, respectively).

Apoptosis of Aorta Vascular wall Smooth Muscle Cells

The model I group had significantly elevated apoptosis of vascular smooth muscle cells compared to model II group or control group ($p<0.05$). No statistical significance existed between model rats without AD formation and control group ($p>0.05$, Figures 9 and 10).

Discussion

AD has relatively higher mortality without surgery. Early medication can retard the rupture of AD[11,12]. Currently, lots of studies have been performed regarding the animal models of AD, whose pathogenesis requires abnormal hemodynamic and weakness of the aorta vascular wall. Studies showed similar results of 0.25% BAPN treated rat AD model as those of clinical results[13,14], with higher formation and mortality rate. BAPN can destruct extracellular matrix of the aorta vascular wall to damage aorta elasticity, anti-tension, and integrity via inhibiting tyrosine oxidase activity,

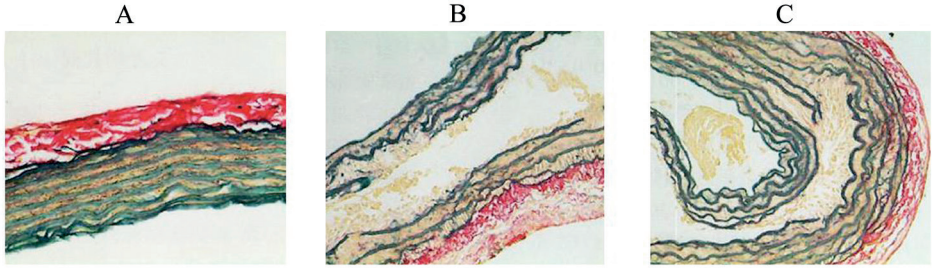

Figure 5. Victoria blue staining of rat aorta (×100). ***A,*** Control group, no AD formation. ***B,*** Model I rats with AD. ***C,*** Model II rats with pseud-AD cavity.

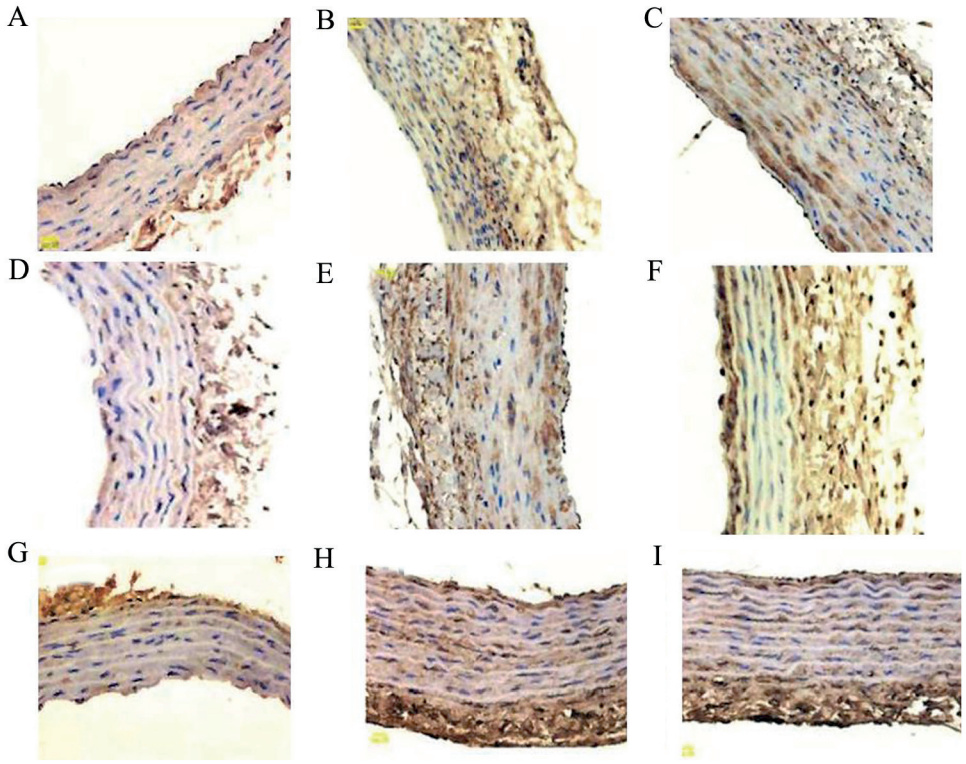

Figure 6. IL-6, IFN-γ and MMP-2 positive expression (×100). ***A, D, G,*** Control group. ***B, E, H,*** Model I group with AD formation. ***C, F, I,*** Model II group without AD formation. ***A, B, C,*** IFN-γ; ***D, E, F,*** MMP-2; ***G, H, I,*** MMP-2.

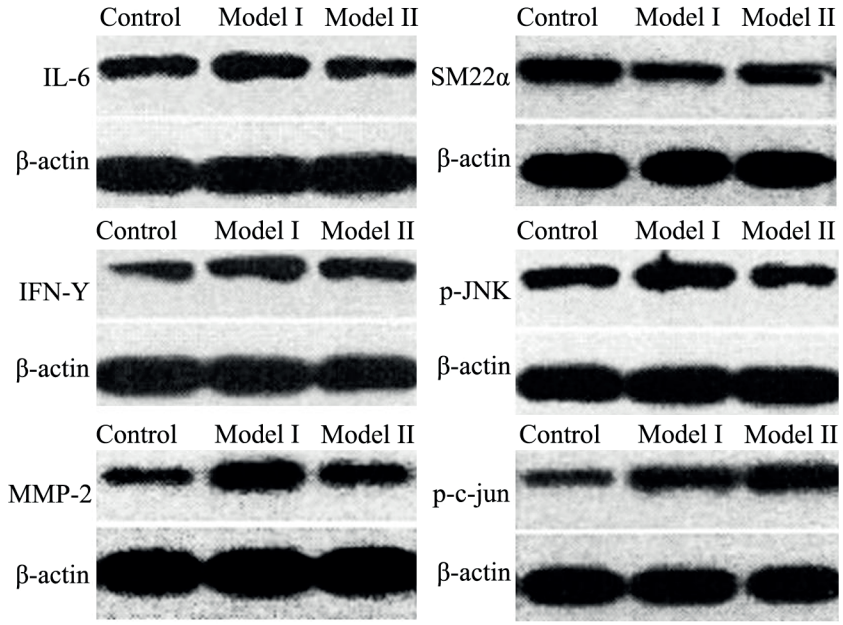

Figure 7. Western blot for aorta expressions of IL-6, IFN-γ, SM22α, MMP-2, p-JNK, and p-c-Jun expression.

interaction between collagen and elastin, thus causing weakness of the aorta vascular wall[15,16]. Elastin occupies about 60% of the thoracic aorta. This study utilized 0.25% BAPN treatment to generate rat AD model and showed about 60% mortality caused by AD rupture. Those model

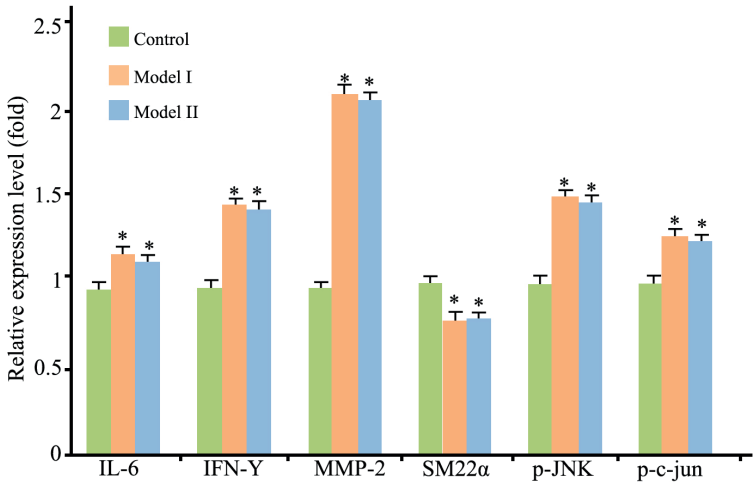

Figure 8. Relative expression level of aorta IL-6, IFN-γ, SM22α, MMP-2, p-JNK and p-c-Jun expression. Model I, complicated with AD; Model II, without AD. *, $p<0.05$ compared to control group; #, $p<0.05$ compared to model II group

rats complicated with AD had significantly higher aorta diameter and aortic media thickness compared to those without AD or control rats. Victoria blue was utilized to observe the structural changes of elastin fiber. Results showed increased elastic fibers gap, disarrangement and fragmentation of elastic fibers, indicating that BAPN treatment damaged integrity of the rat aorta vascular wall, and inhibited effective interaction between collagen and elastin, making inner elastic layer easy to be ruptured, thus lowering resistance against the blood flow, and increasing the risk of artery rupture and AD formation.

AD pathogenesis is associated with degeneration of the aortic media. Moreover, dysfunction of blood supply or hypertension can cause injury to the aortic wall. The defect to the aorta vascular wall and abnormal hemodynamic play important roles in the formation of AD, as weakness of the vascular wall, can cause AD under the effect of abnormal hemodynamic[17,18]. The decrease of effective connection of aorta elastin lamina, deposition of collagen, loss of elastic fiber and apoptosis of smooth muscle cells can all lead to weakness of the aorta vascular wall. A clinical study revealed the close relationship between inflammation and AD formation, as FBN-1 gene knockout mice had inflammatory cell infiltration[19,20]. Currently, no opinions have been agreed regarding whether inflammation causes AD[21,22]. This study established stable AD rat model, in which inflammation in aorta tissue was observed. Results showed significantly elevated IL-6, IFN-γ, MMP-2, p-JNK and p-c-Jun expression in model rats, and lower SM22α expression compared to control group. No significant difference existed of IL-6, IFN-γ, MMP-2, SM22α, p-JNK, and p-c-Jun expression between model rats without AD and control animals, suggesting important roles and possible initiating factor of IL-6, IFN-γ, MMP-2, SM22α, p-JNK, and p-c-Jun in AD formation. Apoptosis of the aorta showed significantly elevated apop-

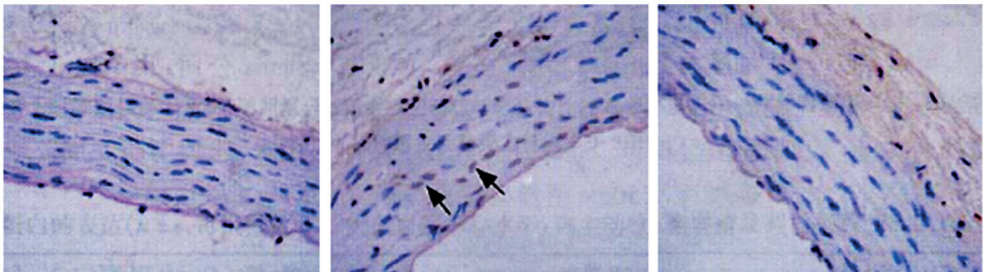

Figure 9. TUNEL staining of aorta vascular wall smooth muscle cells (×100). From left to right, control, model I, model II group.

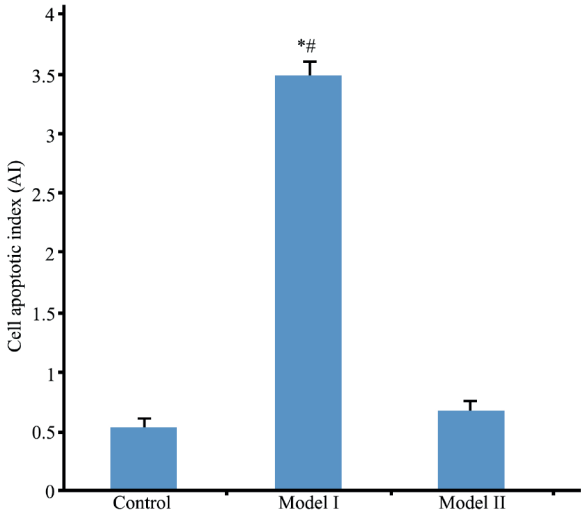

Figure 10. Apoptosis of aorta vascular wall smooth muscle cells. Model I, complicated with AD; Model II, without AD. *, $p<0.05$ compared to control group; #, $p<0.05$ compared to model II group.

tosis of aortic vascular smooth muscle cells in rats with AD compared to those without AD or control ones, and no statistical significant difference between model rats without AD and control group, suggesting that apoptosis of smooth muscle cells in the aorta is a possible result of AD formation. The correlation analysis showed that the expression levels of IL-6 *versus* MMP-2, IL-6 *versus* p-JNK, IFN-γ *versus* MMP-2, IFN-γ *versus* p-c-Jun were significantly positively correlated in model rats with AD, This indicated that IL-6 and IFN-γ might exert their roles via JNK signal pathway, elevating MMP-2 expression, and increasing degradation of the aorta wall matrix. This study only utilized partial factors during AD formation, without reaching 100% formation rate; other potential factors may also affect. This study was thus only a trial study, as further illustration was required for investigating if post-AD inflammation was involved in rupture of elastic fiber and thrombosis inside pseudo cavity.

Conclusions

IL-6, IFN-γ, and MMP-2 expressed highly in AD. During AD formation, IL-6 and IFN-γ may enhance MMP-2 expression and increase extracellular matrix degradation of aorta vascular wall via JNK signal pathway. The apoptosis and phenotype transformation of aortic vascular smooth muscle cells is likewise correlated with AD formation. The exact mechanism needs the further study.

Conflict of interest

The authors declare no conflicts of interest.

References

1) Sakatani A, Doi Y, Kitayama T, Matsuda T, Sasai Y, Nishida N, Sakamoto M, Uenoyama N, Kinoshita K. Pancreaticoduodenal artery aneurysm associated with coeliac artery occlusion from an aortic intramural hematoma. World J Gastroenterol 2016; 22: 4259-4263.
2) Wang G, Zhai S, Li T, Shi S, Zhang Z, Liang K, Fu X, Zhang K, Li K, Li W, Wang B, Zhang D, Lu D. Mechanism and management of retrograde type A aortic dissection complicating TEVAR for type B aortic dissection. Ann Vasc Surg 2016; 32: 111-118.
3) Liao WL, Tan MW, Yuan Y, Wang GK, Wang C, Tang H, Xu ZY. Brahma-related gene 1 inhibits proliferation and migration of human aortic smooth muscle cells by directly up-regulating Ras-related associated with diabetes in the pathophysiologic processes of aortic dissection. J Thorac Cardiovasc Surg 2015; 150: 1292-1301.
4) Yang Y, Wang C, Xu J, Jin T, Xu ZY, Huang SD. BRG1 overexpression in smooth muscle cells promotes the development of thoracic aortic dissection. BMC Cardiovasc Disord 2014; 14: 144.
5) Sano M, Anzai J. The molecular mechanisms contributing to the pathophysiology of systemic inflammatory response after acute aortic dissection. Nihon Rinsho Meneki Gakkai Kaishi 2016; 39: 91-95.
6) Wu MT, Zhang, Bao JM, Zhao ZQ, Lu QS, Feng R, Song C, Zhou J, Jing ZP. Postoperative glucocorticoid enhances recovery after endovascular aortic repair for chronic type B aortic dissection: a single-center experience. BMC Cardiovasc Disord 2016; 16: 59.
7) Wu Z, Ruan Y, Chang J, Li B, Ren W. Angiotensin II is related to the acute aortic dissection complicated with lung injury through mediating the release of MMP9 from macrophages. Am J Transl Res 2016; 8: 1426-1436.
8) Vianello E, Dozio E, Rigolini R, Marroccotrischitta MM, Tacchini L, Trimarchi S, Corsi Romanelli MM. Acute phase of aortic dissection: a pilot study on CD40L, MPO, and MMP-1, -2, 9 and TIMP-1 circulating levels in elderly patients. Immun Ageing 2016; 13: 9.
9) Gomes RZ, Romanek GM, Przybycien M, Amaral DC, Akahane HG. Evaluation of the effect of allopurinol as a protective factor in post ischemia and reperfusion inflammation in Wistar rats. Acta Cir Bras 2016; 31: 126-132.
10) Zhang L, Liao MF, Tian L, Zou SL, Lu QS, Bao JM, Pei YF, Jing ZP. Overexpression of interleukin-1be-

ta and interferon-gamma in type I thoracic aortic dissections and ascending thoracic aortic aneurysms: possible correlation with matrix metalloproteinase-9 expression and apoptosis of aortic media cells. Eur J Cardiothorac Surg 2011; 40: 17-22.

11) Peterss S, Dumfarth J, Rizzo JA, Bonaros N, Fang H, Tranquilli M, Schachner T, Ziganshin BA, Grimm M, Elefteriades JA. Sparing the aortic root in acute aortic dissection type A: risk reduction and restored integrity of the untouched root. Eur J Cardiothorac Surg 2016; 50: 232-239.

12) Gu J, Hu J, Qian H, Shi Y, Zhang E, Guo Y, Xiao Z, Fang Z, Zhong M, Zhang H, Meng W. Intestinal barrier dysfunction: A novel therapeutic target for inflammatory response in acute stanford type A aortic dissection. J Cardiovasc Pharmacol Ther 2016; 21: 64-69.

13) Moulakakis KG, Sfyroeras GS, Papapetrou A, Antonopoulos CN, Mantas G, Kakisis J, Alepaki M, Mylonas SN, Karakitsos P, Liapis CD. Inflammatory response and renal function following endovascular repair of the descending thoracic aorta. J Endovasc Ther 2015; 22: 201-206.

14) Imanaka-yoshida K, Aoki H. Tenascin-C and mechanotransduction in the development and diseases of cardiovascular system. Front Physiol 2014; 5: 283.

15) Xu, CE, Zou CW, Zhang MY, Guo L. Effects of high-dose ulinastatin on inflammatory response and pulmonary function in patients with type-A aortic dissection after cardiopulmonary bypass under deep hypothermic circulatory arrest. J Cardiothorac Vasc Anesth 2013; 27: 479-484.

16) Liu O, Li J, Xin Y, Qin Y, Li H, Gong M, Liu O, Liu YY, Wang XL, Li JR, Zhang HJ. Association of MMP-2 gene haplotypes with thoracic aortic dissection in chinese han population. BMC Cardiovasc Disord 2016; 16: 11.

17) Cifani N, Proietta M, Tritapepe L, Gioia CD, Ferri L, Taurino M, Del Porto F. Stanford-A acute aortic dissection, inflammation, and metalloproteinases: a review. Ann Med 2015; 47: 441-446.

18) Vorkapic E, Lundberg A M, Mäyränpää MI, Eriksson P, Wågsäter D. TRIF adaptor signaling is important in abdominal aortic aneurysm formation. Atherosclerosis 2015; 241: 561-568.

19) Martínalonso M, Garcíaredondo AB, Guo D, Camafeita E, Martínez F, Alfranca A. Deficiency of MMP17/MT4-MMP proteolytic activity predisposes to aortic aneurysm in mice. Circ Res 2015; 117: 13-26.

20) Li Y, Li N, Ma W, Jiang Y, Ma G1, Zhang L. Association between-799C/T single nucleotide polymorphism of the MMP8 promoter region and thoracic aortic dissection. Mol Med Rep 2014; 10: 1857-1862.

21) Cheuk BLY, Chan YC, Cheng SWK. Changes in inflammatory response after endovascular treatment for type B aortic dissection. PLoS One 2011; 7: 448-449.

22) Wang L, Yao L, Guo D, Wang C, Wan B, Ji G, Yang C, Zhang J, Sheng Z, Fu W, Wang Y. Gene expression profiling in acute Stanford type B aortic dissection. Vasc Endovascular Surg 2012; 46: 300-309.